

# Alzheimer Detection Using Wavelet Smoothing Analysis

Jisnu Mohan

PG Student

Department of ECE

Satyam College of Engineering

E-mail : jisnu1990@gmail.com

## Abstract

The spectral graph wavelet transform (SGWT) has recently been developed to compute wavelet transforms of functions defined on non-Euclidean spaces such as graphs. By capitalizing on the established framework of the SGWT, we adopt a fast and efficient computation of a discretized Laplace-Beltrami (LB) operator that allows its extension from arbitrary graphs to differentiable and closed 2-D manifolds (smooth surfaces embedded in the 3-D Euclidean space). This particular class of manifolds are widely used in bio imaging to characterize the morphology of cells, tissues, and organs. They are often discretized into triangular meshes, providing additional geometric information apart from simple nodes and weighted connections in graphs.

**Keywords:** Hippocampal shape, Laplace-Beltrami operator, signal processing on surfaces, two-dimensional (2-D) manifold

## 1 INTRODUCTION

In comparison with the SGWT, the wavelet bases constructed with the LB operator are spatially localized with a more uniform “spread” with respect to underlying curvature of the surface. In our experiments, we first use synthetic data to show that traditional applications of wavelets in smoothing and edge detection can be done using the wavelet bases constructed with the LB operator. Second, we show that multi-resolution capabilities of the proposed framework are applicable in the classification of Alzheimer's patients with normal subjects using hippocampal shapes.

WAVELET analysis has been applied widely over a variety of cross-disciplinary applications, and has achieved considerable success, particularly in signal processing, data compression, and pattern recognition problems. With the progressive collection of large network datasets, such as social networks and brain networks, and the development of statistical techniques for on-Euclidean spaces, the study of wavelet analysis in these irregular spaces hopes to exploit the parsimonious and multi-resolution capabilities of the classical wavelet transform, providing a more compact representation of large datasets and focused analyses of complex networks at different levels of detail. In particular, several extensions of the wavelet transform defines formally the construction of wavelets on smooth, compact, differentiable manifolds—an important class of manifolds widely used in mathematical models of bio imaging and its related statistical analyses. Thus, to actually verify essential self-adjointness of a differential operator, one typically has to first solve a PDE (such as the wave, Schrödinger, heat, or Helmholtz equation) by some non-spectral method (e.g. by a contraction mapping argument, or a perturbation argument based on an operator already known to be essentially self-adjoint).

Once one can solve one of the PDEs, then one can apply one of the known converse spectral theorems to obtain essential self-adjointness, and then by the forward spectral theorem one can then solve all the other PDEs as well. But there is no getting out of that first step, which requires some input (typically of an ODE, PDE, or geometric nature) that is external to what abstract spectral theory can provide. For instance, if one wants to establish essential self-adjointness of the Laplace-Beltrami operator

$\{L = -\Delta_g\}$  on a smooth Riemannian manifold  $\{(M, g)\}$  (using  $\{C^\infty_c(M)\}$  as the domain space), it turns out (under reasonable regularity hypotheses) that essential self-adjointness is equivalent to geodesic completeness of the manifold, which is a global ODE condition rather than a local one: one needs geodesics to continue indefinitely in order to be able to (unitarily) solve PDEs such as the wave equation, which in turn leads to essential self-adjointness. (Note that the domains  $\{(0, 1)\}$  and  $\{(0, +\infty)\}$  in the previous examples were not geodesically complete.) For this reason, essential self-adjointness of a differential operator is sometimes referred to as quantum completeness (with the completeness of the associated Hamilton-Jacobi flow then being the analogous classical completeness).

In these notes, I wanted to record (mostly for my own benefit) the forward and converse spectral theorems, and to verify essential self-adjointness of the Laplace-Beltrami operator on geodesically complete manifolds. This is extremely standard analysis (covered, for instance, in the texts of Reed and Simon), but I wanted to write it down myself to make sure that I really understood this foundational material properly. spectral shape analysis relies on the spectrum (eigenvalues and/or eigenfunctions) of the Laplace-Beltrami operator to compare and analyze geometric shapes. Since the spectrum of the Laplace-Beltrami operator is invariant under isometries, it is well suited for the analysis or retrieval of non-rigid shapes, i.e. bendable objects such as humans, animals, plants, etc.

The solutions are the eigenfunctions  $\phi_i$  (modes) and corresponding eigenvalues  $\lambda_i$ , representing a diverging sequence of positive real numbers. The first eigenvalue is zero for closed domains or when using the Neumann boundary condition. For some shapes, the spectrum can be computed analytically (e.g. rectangle, flat torus, cylinder, disk or sphere). For the sphere, for example, the eigenfunctions are the spherical harmonics.

The most important properties of the eigenvalues and eigenfunctions are that they are isometry invariants. In other words, if the shape is not stretched (e.g. a sheet of paper bent into the third dimension), the spectral values will not change. Bendable objects, like animals, plants and humans, can move into different body postures with only minimal stretching at the joints. The resulting shapes are called near-isometric and can be compared using spectral shape analysis. However, the isometric deformation of surfaces in 3D in the strict sense are rigid transformations. To characterize the actual deformation undergoing for the interest of nonrigid shape analysis, smooth deformations are introduced as an alternative family of deformation to isometry, where eigenvalues are allowed to perturb with finite error bounds.

### 1.1 Review On The Spectral Graph Wavelet Transform

Wavelets are basis functions that are scaled and shifted variants of a mother wavelet, defined over the continuous domain of an admissible function. For instance, a “mother” wavelet, defined over continuous time, is translated times and scaled times, to produce the  $n$ th basis, bearing the general form (1) For any given signal, the wavelet coefficient, at scale and location, is denoted as and constructed with an inner product (2) Consider now a topologically complex domain,  $\mathcal{G}$ , which, in general, may not be Euclidean. In the SGWT [4], a given function is defined on the vertices of a weighted graph, where  $V$  is a set of vertices,  $E$  is a set of edges, and  $w$ , or an assignment of one positive weight for every edge. A graph Laplacian operator is defined as, where  $D$  and  $A$  are the degree and adjacency matrices of  $\mathcal{G}$ , respectively. Since  $L$  is real and symmetric, it has a complete set of orthonormal eigenvectors  $\phi_i$ , for  $i = 1, 2, \dots$ , with associated eigenvalues  $\lambda_i$ , such that (3) The graph Fourier transform of  $f$  is then defined by  $\hat{f}(\lambda_i) = \langle f, \phi_i \rangle$  (4) As each vertex on the graph is discrete, there is no natural way to define a scaled wavelet basis. This problem was circumvented by working in a spectral graph domain, where a wavelet-generating kernel, analogous to a band-pass filter, was shifted along the spectrum. As the band pass filter journeys up from the low to the high frequency bands, the “spread” of the wavelet bases becomes increasingly localized on the graph domain. In [4], the wavelet basis at the given location and scale, is defined as (5) For a function defined on the graph, its corresponding wavelet coefficient at that particular scale,  $s$ , and location is then computed with the inner product (6) The low frequency content of the graph, i.e., when  $\lambda_i$  is close to 0, is captured separately with another real-valued function, that satisfies the conditions and as  $\phi_0$ . The basis constructed from  $\phi_0$  is analogous to the scaling function in the set-up of a classical wavelet transform.

### 1.1.1 Discretization

Geometric shapes are often represented as 2D curved surfaces, 2D surface meshes (usually triangle meshes) or 3D solid objects (e.g. using voxels or tetrahedra meshes). The Helmholtz equation can be solved for all these cases. If a boundary exists, e.g. a square, or the volume of any 3D geometric shape, boundary conditions need to be specified.

Several discretizations of the Laplace operator exist (see Discrete Laplace operator) for the different types of geometry representations. Many of these operators do not approximate well the underlying continuous operator.

### 1.1.2 Global point signature (GPS)

The global point signature[6] at a point  $x$  is a vector of scaled eigenfunctions of the Laplace–Beltrami operator computed at  $x$  (i.e. the spectral embedding of the shape). The GPS is a global feature in the sense that it cannot be used for partial shape matching. The heat kernel signature makes use of the eigen-decomposition of the heat kernel:

$$h_t(x,y) = \sum_{i=0}^{\infty} \exp(-\lambda_i t) \phi_i(x) \phi_i(y).$$

For each point on the surface the diagonal of the heat kernel  $h_t(x,x)$  is sampled at specific time values  $t_j$  and yields a local signature that can also be used for partial matching or symmetry detection.

### 1.1.3 Spectral Matching

The spectral decomposition of the graph Laplacian associated with complex shapes (see Discrete Laplace operator) provides eigenfunctions (modes) which are invariant to isometries. Each vertex on the shape could be uniquely represented with a combinations of the eigenmodal values at each point, sometimes called spectral coordinates:

$$s(x) = (\phi_1(x), \phi_2(x), \dots, \phi_N(x)) \text{ for vertex } x.$$

Spectral matching consists of establishing the point correspondences by pairing vertices on different shapes that have the most similar spectral coordinates. Early work [8][9][10] focused on sparse correspondences for stereoscopy.

## 2 LITERATURE SURVEY

### Wavelet Based Multi-Scale Shape Features On Arbitrary Surfaces For Cortical Thickness Discrimination

Hammond recently developed the spectral graph wavelet transform (SGWT) that is based on the graph-Fourier transform. It is implemented through the graph Laplacian by first constructing a surrogate spectral domain and then introducing a wavelet generating kernel in this spectral domain for the purpose of the spectral localization. It has found applications in many disciplines, particularly in neuroimaging research. For instance, multi-scale wavelet coefficients generated from the SGWT were concatenated and employed as high-dimensional projections of signals defined on arbitrary graph domains. This has been shown to improve statistical power for detecting subtle differences in cortical thickness between normal subjects and patients with Alzheimer's disease. In addition, the SGWT construction and its desirable properties can be varied through a choice of wavelet-generating kernels. For instance, a kernel, analogous to Meyer wavelets, builds an energy-conserving Parseval frame. As shown in [6], this kernel captures coherent brain activity of fMRI data with varying efficiencies, dependent on how well the wavelet transform was suited to the specific brain simulation. In addition, SGWT was also used as a segmentation scheme for 3-D shapes at different scales of a wavelet generating kernel].

### Wavelet Transform On Manifolds: Old And New Approaches

Morphometric studies of brain structures have classically been based on volume measurements. More recently, shape studies of gray matter brain structures have become popular. Methodologies for shape comparison may be divided into global and local shape analysis approaches. While local shape comparisons [1], [2], [3] yield powerful, spatially localized results that are relatively straightforward to interpret, they usually rely on a number of preprocessing steps. In particular, one-to-one correspondences between surfaces need to be established, shapes need to be registered and resampled, possibly influencing shape comparisons. While global shape comparison cannot spatially localize shape changes, global approaches may be formulated with a significantly reduced number of assumptions and preprocessing steps, staying as true as possible to the original data.

### Global Medical Shape Analysis Using The Volumetric Laplace Spectrum

In particular, the paper focuses on the volumetric Laplace spectrum of three-dimensional solids. Previous approaches for global shape analysis in medical imaging include the use of invariant moments [8], the shape index [9], and global shape descriptors based on spherical harmonics [10]. The proposed

methodology based on the Laplace-Beltrami spectrum differs in the following ways from these previous approaches: - It works directly for any Riemannian manifold, whereas spherical harmonics based methods require spherical representations, and invariant moments do not easily generalize to arbitrary Riemannian manifolds. It may be used to analyze surface, solids, non-spherical objects, etc. in different representations. - Only minimal preprocessing of the data is required. Three dimensional volume data may be represented by its boundary surface, separating the object interior from its exterior or by the volume itself (a volumetric, region-based approach).

## 2.1 PROBLEM DEFINITION

While the SGWT is attractive, its construction based on the graph Laplacian, captures only information such as the nodes and edges of an arbitrary graph. However, the geometry of surfaces in many bio imaging applications, such as 3-D heart models, blood vessels, and brain cortical surfaces, is important for understanding biological processes. It is hence essential to incorporate geometric information of these biological surfaces into the wavelet construction. In this paper, we are primarily interested in extending the SGWT developed by onto differentiable, compact and boundary-less two-manifolds (smooth and closed surfaces embedded in the 3-D Euclidean space). In general, for the ease of computation, these surfaces are often discretized into triangular meshes, allowing their interpretation as graphs with discrete nodes and edges. By capitalizing on the established framework of the SGWT, we hope to replace the graph Laplacian with a discretized Laplace-Beltrami operator that captures geometric information such as the intrinsic curvature of the underlying surfaces in addition to the nodes and edges

## 3 PROPOSED SYSTEM

### 3.1 Methodology

Analogous to the Eigen functions of the graph Laplacian, which are used to construct the spectral domain of an arbitrary graph, the Eigen functions of the Laplace-Beltrami operator can be used to define the spectral domain of an arbitrary 2-D manifold surface. These Eigen functions form an informative set of functions that incorporate the intrinsic geometry of the manifold with different degrees of sensitivity along the spectrum. They are widely used in many applications, such as signal processing on manifolds, shape segmentation and classification. For instance, Eigen functions of the Laplace-Beltrami operator, which were used to smooth functional signals on brain cortical surfaces, were also employed as global shape descriptors to capture the differences in caudate shapes between controls and schizotypal patients. Geometric information incorporated in the Eigen functions is also useful in constructing other operators, such as heat kernel for smoothing functions defined over the two-manifolds. Following the wide application of the Laplace-Beltrami operator in the medical and computer vision fields, robust numerical methods of computing a discretized Laplace-Beltrami operator have attracted a fair amount of attention. In this paper, we constructed the Laplace-Beltrami operator as a discrete geometric operator so as to make use of the fast polynomial approximation developed in . Effects of user-defined parameters used in the framework will also be investigated. In Section IV, we demonstrate the advantages of our spectral wavelets over the SGWT and apply the wavelet transform, first on simulated shapes, and then on real data such as the cortical thickness of the brain. Lastly, we show an application of the spectral wavelet transform wherein the classification rates between control and Alzheimer's patients, using hippocampal shapes, can be improved.

#### 3.1.1 Mathematical Model

Wavelets are basis functions that are scaled and shifted variants of a mother wavelet , defined over the continuous domain of an admissible function, . For instance, a “mother” wavelet , defined over continuous time, is translated times and scaled times, to produce the  $j$ th basis,

$$\psi_{j,k}(t) = \frac{1}{j} \psi \left( \frac{t-k}{j} \right), \quad j > 0, k \in \mathbb{R}.$$

For any given signal  $f$ , the wavelet coefficient  $W_f(j, k)$ , at scale  $j$  and location  $k$ , is denoted as and constructed with

$$W_f(j, k) = \int_{-\infty}^{\infty} \psi_{j,k}(t) f(t) dt.$$

an inner product

Consider now a topologically complex domain,  $\Omega$ , which, in general, may not be Euclidean. In the SGWT [4], a given function is defined on the vertices of a weighted graph  $G$ , where  $V$  is a set of vertices,  $E$  is a set of edges, and  $w$ , or an assignment of one positive weight for every edge. A graph Laplacian operator is defined as  $L = D - A$ , where  $D$  and  $A$  are the degree and adjacency matrices of  $G$ , respectively. As the band pass filter journeys up from the low to the high frequency bands, the “spread” of the wavelet bases becomes increasingly localized on the graph domain. In [4], the wavelet basis at the given location and scale  $j$ , is defined as

$$\psi_{j,n}(m) = \sum_{l=0}^{N-1} g(j\lambda_l) \chi_l(n) \chi_l(m).$$

The low frequency content of the graph, i.e., when  $j$  is close to 0, is captured separately with another real-valued function  $\phi$ , that satisfies the conditions  $\phi(0) = 1$  and  $\phi(1) = 0$ . The basis constructed from  $\phi$  is analogous to the scaling function in the set-up of a classical wavelet transform.

Coefficients of a cubic polynomial are determined by the continuity constraints  $\phi(0) = 1$  and  $\phi(1) = 0$ . The discretized wavelet scales, which we will now denote as  $j$ , have to be determined from the upper bound of the spectrum of the Laplace-Beltrami operator. The minimum and maximum scales  $j_{\min}$  and  $j_{\max}$  are computed as  $j_{\min} = \lceil \log_2(\lambda_{\max}) \rceil$  and  $j_{\max} = \lceil \log_2(\lambda_{\min}) \rceil$ , and the remaining are spaced logarithmically in between. Note that  $\lambda_{\min}$  is a user-defined parameter and determines the lower bound of the spectrum. We will discuss further in Section III-D1. By sharing the same wavelet-generating kernel as the spectral graph wavelets, we are always assured of spectral localization, as that has been specified within the construction of  $\psi$ .

### 3.2 Implementation

1) Choosing  $\lambda_{\min}$ : The construction of the wavelet basis is artificially orchestrated by the design of kernel  $\psi$ , which in turn, moves along the spectral domain of the underlying structure as scale changes. By spacing out the scales along the spectrum, we control the size of the “spread” of the wavelet bases, which is often dependent on the nature of our application. For instance, a large  $\lambda_{\min}$  corresponds to a large “spread” and acts inadvertently as a smoothing function, while a small  $\lambda_{\min}$  detects edge or high frequency differences in the function defined on the surface. Since we fix the upper bound of the spectrum at  $\lambda_{\max}$ , the user-defined parameter determines the lower bound, or essentially, the area of influence of  $\psi$  at the largest  $j$ , the effects of  $\lambda_{\min}$  on the “spread” of  $\psi$  could be seen from a range of 2000 to 50 000, at a fixed scale  $j$ .

2) Choosing  $N$ : Due to the computational intensity of the eigenvalues and Eigen functions for densely-sampled surfaces, we employ the approximation of using Chebyshev polynomials [4]. This requires us to determine another free parameter that specifies the number of polynomial terms in the Chebyshev expansion. The sequence of Chebyshev polynomials, used Effects of the change of  $N$  on the “spread” of the wavelet basis. increases from left to right. Triangular mesh has 81 920 faces and 40 962 vertices. These panels show the fifth wavelet basis  $\psi_{j,n}$ . Effects of  $N$  on wavelet bases. wavelet basis generated based on the Laplace-Beltrami operator at three scales (decreasing from left to right along each row) at a fixed location. From top to bottom row, the user defined parameter increases from 20 to 100 to 500, .frequently in numerical analyses, can be defined recursively upto a degree  $N$ . Thus one needs suitable techniques for analyzing such data. In the spherical case, the Fourier transform amounts to an expansion in spherical harmonics, whose support is the whole sphere. Fourier analysis on the sphere is thus global and cumbersome. Therefore many different methods have been proposed to replace it with some sort of wavelet analysis.

### Implementation of Spectral Wavelet Transform

Given , we want to compute .

Step 1: Initialization

Step 2: Compute the Laplace-Beltrami operator matrix

Step 3: Compute

Step 4: Specify the wavelet generating kernel operator .

Step 5: Implement the spectral wavelet transform in (23) to obtain . For dense meshes, the polynomial approximation scheme in [4] is recommended

### 3.3 Expected Result

This study explains the various characteristics and properties of the aluminium alloy. By means the literature survey it is well clear that the aluminium alloy is best suitable for its properties. This project describes the latest and strongest alloy automobile leaf spring. The new alloy, containing 90% aluminium & 7% zinc is an inexpensive substitute for steel.

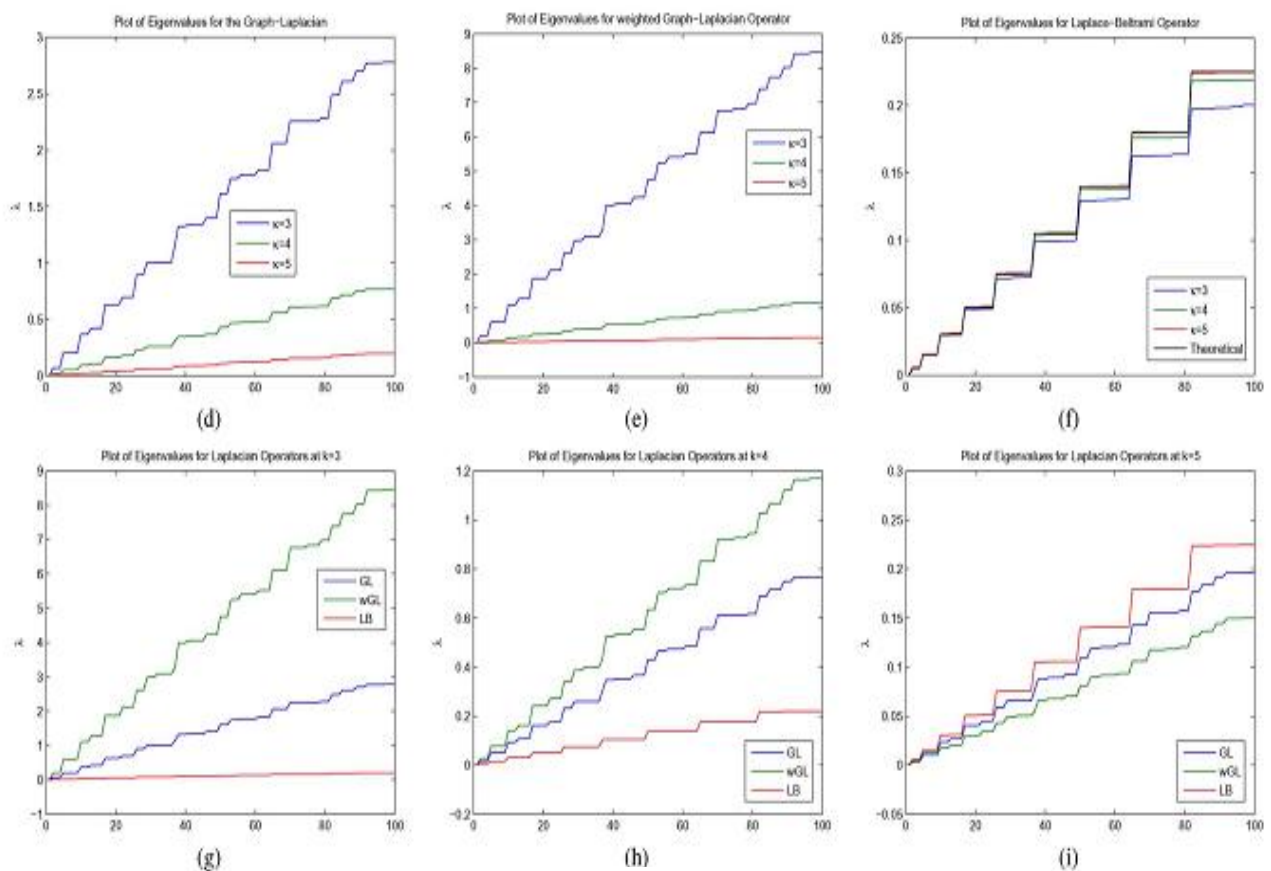
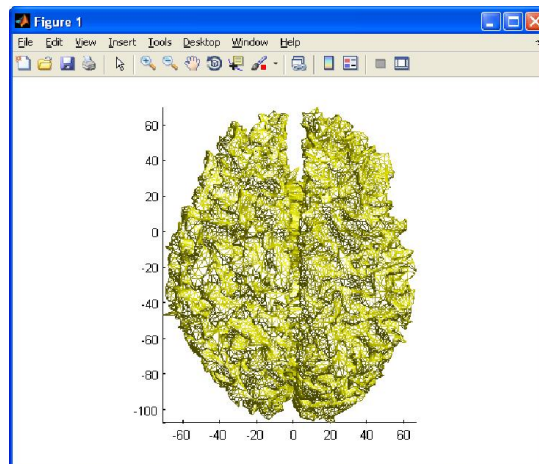


Figure 3.1: Different Sampling Densities

While this transformation has biological significance, as shown in the classification experiment between the Alzheimer's and normal subjects, the high-dimensionality of the corresponding wavelet coefficients could result in inconveniences for data storage or statistical analyses. The development of a sparse representation from dictionary of wavelet bases could be helpful in defining a low-dimensional representation of functions defined on manifolds, without resorting to common linear data reduction methods such as the PCA or multi-dimensional scaling.

## 4 RESULT



*Figure 4.1: Input Image*

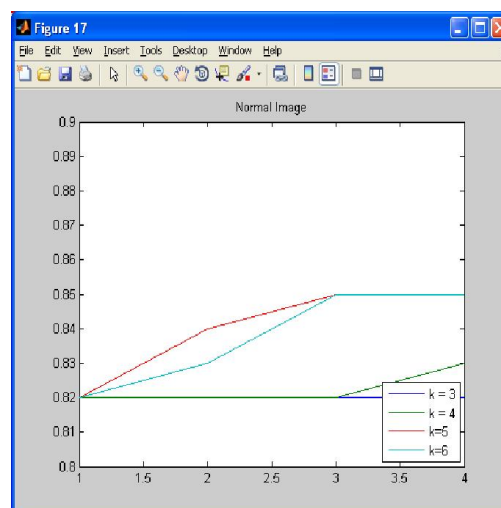


*Figure 4.2: Normal Brain Image*

## 5 CONCLUSION

We now show that the wavelet bases generated from the discretized Laplace-Beltrami operators are localized in the spatial domain. To prove this, we mimic closely the proof for the spatial localization

property of the SGWT. First, we will describe a new corollary (Corollary 2) to link the discretized Laplace-Beltrami with the graph Laplacian, which is needed in the proof of Corollary 1. Corollary 2: Let  $\Delta$  be the discretized Laplace-Beltrami operator of a differentiable, closed manifold surface, and computed based on (19). Let  $n$  be an integer such that for any pair of vertices  $v_i, v_j$ , where  $n$  is the total number of rings containing  $v_i$  with respect to  $v_j$ , and  $i$  is an index numbering from 1 to  $n$ . If  $k$  is an integer, then  $k \leq n$ . There are many ways to define a discretized Laplace-Beltrami (LB) operator, and it is not clear if all such schemes could apply to the given formulation of spectral wavelets. With corollary 2, we demonstrated the important similarity established between the graph Laplacian and the discretized Laplace-Beltrami operator detailed in Section III-A. The minimum number of edges of any path connecting points  $v_i$  and  $v_j$  in a graph would be identical to  $|k_i - k_j|$ , where  $k_i, k_j$  whenever the same set of one-ring neighbors is used for both Laplacians, i.e., if edges are required to join two points, one of the points would then be in the  $k$ -ring of the other.

In the future work the Feature kernel regression and diffusion smoothing share identical FEM discretization. The flexibility of the parametric model enabled us to establish the mathematical equivalence of kernel regression, diffusion smoothing and diffusion wavelets.

## REFERENCES

- [1] R. R. Coifman and M. Maggioni, "Diffusion wavelets," *Appl. Comput. Harmon. Anal.*, vol. 21, no. 1, pp. 53–94, 2006.
- [2] D. Geller and A. Mayeli, "Continuous wavelets on compact manifolds," *Mathematische Zeitschrift*, vol. 262, no. 4, pp. 895–927, 2009.
- [3] J.-P. Antoine, D. Roca, and P. Vandergheynst, "Wavelet transform on manifolds: Old and new approaches," *Appl. Comput. Harmon. Anal.* vol. 28, no. 2, pp. 189–202, 2010 [Online]. Available: <http://www.sciencedirect.com/science/article/pii/S1063520309001134>
- [4] D. K. Hammond, P. Vandergheynst, and R. Gribonval, "Wavelets on graphs via spectral graph theory," *Appl. Comput. Harmon. Anal.*, vol. 30, no. 2, pp. 129–150, 2011.
- [5] W. H. Kim, D. Pachauri, C. Hatt, M. K. Chung, S. Johnson, and V. Singh, "Wavelet based multi-scale shape features on arbitrary surfaces for cortical thickness discrimination," in *Adv. Neural Inf. Process. Syst.*, 2012, pp. 1250–1258.
- [6] N. Leonardi and D. Van De Ville, "Wavelet frames on graphs defined by fMRI functional connectivity," in *Proc. IEEE Int. Symp. Biomed. Imag., From Nano to Macro*, 2011, pp. 2136–2139.
- [7] W. H. Kim, M. K. Chung, and V. Singh, "Multi-resolution shape analysis via non-Euclidean wavelets: Applications to mesh segmentation and surface alignment problems," *Proc. IEEE Comput. Vis. Pattern Recognit. Conf.*, pp. 2139–2146, 2013.
- [8] W.H.Kim, N.Adhuru, M.K.Chung, S.Charchut, J.J.GadElkarim, L. Altshuler, T. Moody, A. Kumar, V. Singh, and A. D. Leow, "Multi-resolutional brain network filtering and analysis via wavelets on non-Euclidean space," in *Medical Image Computing and Computer-Assisted Intervention-MICCAI*. Berlin, Germany: Springer, 2013, pp. 643–651.
- [9] A. Qiu, D. Bitouk, and M. I. Miller, "Smooth functional and structural maps on the neocortex via orthonormal bases of the laplace-beltrami operator," *IEEE Trans. Med. Imag.*, vol. 25, no. 10, pp. 1296–1306, Oct. 2006.
- [10] M. Niethammer, M. Reuter, F.-E. Wolter, S. Bouix, N. Peinecke, M.-S. Koo, and M.E.Shenton, "Global medical shape analysis using the Laplace-Beltrami spectrum," in *Medical Image Computing and Computer-Assisted Intervention-MICCAI*. New York: Springer, 2007, pp. 850–857.
- [11] S. Seo, M. K. Chung, and H. K. Vorperian, "Heat kernel smoothing using Laplace-Beltrami eigen functions," in *Medical Image Computing and Computer-Assisted Intervention-MICCAI*. New York: Springer, 2010, pp. 505–512.
- [12] M. Meyer, M. Desbrun, P. Schröder, and A. H. Barret al., "Discrete differential-geometry operators for triangulated 2-manifolds," *Visualizat. Math.* III, , pp. 35–57, 2003.
- [13] M. Reuter, S. Biasotti, D. Giorgi, G. Patané, and M. Spagnuolo, "Discrete Laplace-Beltrami operators for shape analysis and segmentation," *Comput. Graph.*, vol. 33, no. 3, pp. 381–390, 2009.



- [14] U. Pinkall and K. Polthier, "Computing discrete minimal surfaces and their conjugates," *Exp. Math.*, vol. 2, no. 1, pp. 15–36, 1993.
- [15] M. Reuter, F.-E. Wolter, and N. Peinecke, "Laplace-spectra as fingerprints for shape matching," in *Proc. 2005 ACM Symp. Solid Phys. Model.*, 2005, pp. 101–106.